JOC Article

Solvent-Controlled Photoinduced Electron Transfer between Porphyrin and Carbon Nanotubes

Peng Liang, Heng-Yi Zhang, Zhi-Lin Yu, and Yu Liu*

Department of Chemistry, State Key Laboratory of Elemento-Organic Chemistry, Nankai University, Tianjin 300071, P. R. China

yuliu@nankai.edu.cn

Received November 6, 2007

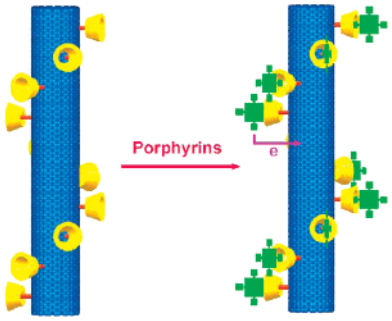

β-Cyclodextrin (β-CD)-modified multiwalled carbon nanotubes (MWCNTs) were successfully prepared by reaction of surface-bound carboxylic chloride groups of MWCNTs with aminoethyleneamino-deoxy-β-CD (ENCD) and comprehensively characterized by FTIR, Raman, and X-ray photoelectron spectroscopy and thermogravimetric and differential thermal analysis. The β-CD-modified MWCNTs (ENCD-MWCNTs) are highly water-soluble, with a solubility of ca. 9.0 mg·mL^{-1}. Furthermore, the photoinduced electron transfer (PET) process between tetrakis(4-carboxyphenyl)porphyrin (TCPP) and ENCD-MWCNTs was investigated by means of fluorescence, fluorescence decay, transient absorption spectroscopy, and cyclic voltammetry. Obvious quenching processes were observed upon addition of both MWCNT-COOH and ENCD-MWCNTs to the aqueous solutions of TCPP, indicating that the PET process between TCPP and carbon nanotubes takes place upon irradiation. When 1-adamantane acetic acid was added to the aqueous solutions of TCPP/MWCNT-COOH and TCPP/ENCD-MWCNTs, respectively, the former fluorescence remains, while the latter fluorescence recovers. On the contrary, the fluorescence intensity of TCPP in the DMF solution was hardly decreased upon addition of ENCD-MWCNTs, whereas its fluorescence was quenched in the presence of MWCNT-COOH. The observations indicate that the CD cavities play a vital role on the control of the PET process.

Introduction

Carbon nanotubes (CNTs) are essentially sheets of carbon atoms arranged in hexagons that curl into a tube. Possessing unique electrical and electronic properties, wide electrochemical stability windows, and high surface areas, CNTs have attracted considerable attention for energy conversion devices and light-harvesting assemblies.[1−3] However, basic research at the molecular level and further applications have been hampered by the difficulties of processing these highly intractable carbon nanostructures and of obtaining homogeneous dispersions in common solvents. In order to improve their solubilities, there have been covalent[4] and noncovalent[4a,d,h,5] strategies for functionalization of carbon nanotubes involving reactions with organic or polymeric molecules. Because these materials have strong absorbance cross sections especially in the visible region of the solar spectrum, a great deal of effort has been devoted to studies of electron-transfer reactions between porphyrins and

(1) (a) Dresselhaus, M. S.; Dresselhaus, G.; Avouris, P. *Carbon Nanotubes: Synthesis, Structure, Properties and Applications*; Springer-Verlag: Berlin, Heidelberg, 2001. (b) Endo, M.; Iijima, S.; Dresselhaus, M. S. *Carbon Nanotubes*; Elsevier Science Ltd.: Oxford, 1996. (c) Reich, S.; Thomsen, C.; Maultzsch, J. *Carbon Nanotubes. Basic Concepts and Physical Properties*; Wiley-VCH: Weinheim, 2004. (d) Harris, P. J. F. *Carbon Nanotubes and Related Structures: New Materials for the Twenty-First Century*; Cambridge University Press: Cambridge, 2001.

10.1021/jo702400k CCC: $40.75
Published on Web 02/21/2008

SCHEME 1

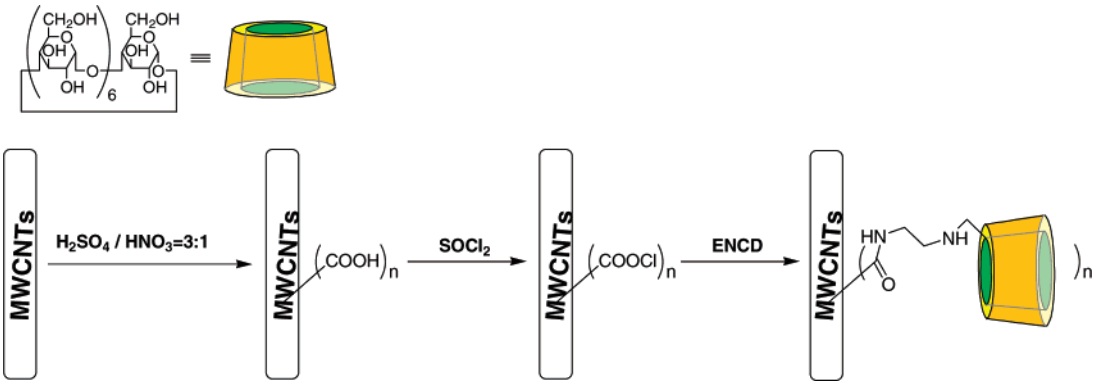

CNTs. The latter has resulted in a class of supramolecular nanoassemblies for generating singlet excited energy and its conversion to chemical energy.[6,7] Both covalent and noncovalent methods have been explored to integrate porphyrins with CNTs. In the latter method, in addition to the face-to-face $\pi-\pi$ interactions of porphyrins with CNTs,[8] electrostatic interactions between the functional groups (such as pyrene derivatives,[9] poly(sodium 4-styrenesulfonate)[10]) attached to the surface of CNTs and charged porphyrins can help to immobilize porphyrins onto CNTs. This has led to the realization of electron-transfer reactions of intra-nanohybrids. Here, we prepared a β-cyclodextrin (β-CD)-modified multiwalled carbon nanotube (MWCNTs), which has been comprehensively investigated by FTIR, Raman, and X-ray photoelectron spectroscopy (XPS) and thermogravimetric (TG) and differential thermal analysis (DTA). The material has greatly increased water solubility (9.0 mg/mL) compared to that of the uncomplexed MWCNTs. Importantly, β-CDs can bind and release tetrakis(4-carboxyphenyl)porphyrin (TCPP) in aqueous solution and organic solvents, respectively, and in doing so can significantly mediate the photoinduced electron transfer (PET) process between TCPP and MWCNTs.

Results and Discussion

Synthesis. The surface-bound carboxylic acid groups of MWCNTs (MWCNT-COOH) were prepared by reaction of MWCNTs with sulfuric acid/nitric acid solutions. After MWCNT-COOH was transformed into MWCNT-COCl, 6^{I}-(2-aminoethylene amino)-6^{I}-deoxy-β-cyclodextrin (ENCD) was added to the MWCNT-COCl DMF solution, a black solid consisting of the ENCD-MWCNTs conjugate was obtained (Scheme 1). We also attempted the reaction of the pristine MWCNTs with ENCD under the same conditions, but no product between MWCNTs and ENCD was obtained, indicating that the ENCDs do not react with the sidewall carbons but form an amide linkage with the COOH group to the sidewall.

FT-IR and Raman Spectra. The FTIR spectrum of ENCD-MWCNTs shows characteristic vibrations centered at 1665 and 1620 cm^{-1}, which should be attributed to the amide carbonyl group. Raman spectroscopy[11] is a useful tool for the characterization of structure changes in CNTs. Raman spectra of pristine MWCNTs, MWCNT-COOH, and ENCD-MWCNTs with excitation at 785 nm are reported in Figure 1. Raman spectra of the pristine MWCNTs show two prominent bands at about 1300−1400 (D-band) and 1500−1600 (G-band) cm^{-1}. The D-band indicates, as usual for carbon nanostructures, the density of defects and can be used for monitoring the process of functionalization that transforms sp^2 to sp^3 sites. Comparing to the pristine MWCNTs, we note that the D-band of MWCNT-

(2) (a) Special issue on carbon nanotubes: Haddon, R. C. *Acc. Chem. Res.* **2002**, *35*, 997−997. (b) Terrones, M. *Annu. Rev. Mater. Res*. **2003**, *33*, 419−501. (c) Martín, N.; Sánchez, L.; Illescas, B.; Pérez, I. *Chem. Rev.* **1998**, *98*, 2527−2548. (d) Diederich, F.; Gomez-Lopez, M. *Chem. Soc. Rev*. **1999**, *28*, 263−277. (e) Guldi, D. M.; Prato, M. *Acc. Chem. Res.* **2000**, *33*, 695−703. (f) Gust, D.; Moore, T. A.; Moore, A. L. *Acc. Chem. Res.* **2001**, *34*, 40−48.

(3) (a) Imahori, H.; Sakata, Y. *Adv. Mater*. **1997**, *9*, 537−546. (b) Ago, H.; Petritsch, K.; Shaffer, M. S. P.; Windle, A. H.; Friend, R. H. *Adv. Mater.* **1999**, *11*, 1281−1284. (c) Bhattacharyya, S.; Kymakis, E.; Amaratunga, G. A. J. *Chem. Mater*. **2004**, *16*, 4819−4823. (d) Landi, B. J.; Castro, S. L.; Ruf, H. J.; Evans, C. M.; Bailey, S. G.; Raffaelle, R. P. *Sol. Energy Mater. Sol. Cells* **2005**, *87*, 733−746. (e) Rahman, G. M. A.; Guldi, D. M.; Cagnoli, R.; Mucci, A.; Schenetti, L.; Vaccari, L.; Prato, M. *J. Am. Chem. Soc.* **2005**, *127*, 10051−10057. (f) Raffaelle, R. P.; Landi, B. J.; Harris, J. D.; Bailey, S. G.; Hepp, A. F. *Mater. Sci. Eng., B* **2005**, *116*, 233−243. (g) Guldi, D. M.; Rahman, G. M. A.; Sgobba, V.; Kotov, N. A.; Bonifazi, D.; Prato, M. *J. Am. Chem. Soc.* **2006**, *128*, 2315−2323.

(4) (a) Hirsch, A. *Angew. Chem., Int. Ed.* **2002**, *41*, 1853−1859. (b) Sun, Y.-P.; Fu, K.; Lin, Y.; Huang, W. *Acc. Chem. Res.* **2002**, *35*, 1096−1104. (c) Niyogi, S.; Hamon, M. A.; Hu, H.; Zhao, B.; Bhowmik, P.; Sen, R.; Itkis, M. E.; Haddon, R. C. *Acc. Chem. Res.* **2002**, *35*, 1105−1113. (d) Tasis, D.; Tagmatarchis, N.; Georgakilas, V.; Prato, M. *Chem. Eur. J.* **2003**, *9*, 4000−4008. (e) Banerjee, S.; Hemraj-Benny, T.; Wong, S. S. *Adv. Mater.* **2006**, *17*, 17−29. (f) Balasubramanian, K.; Burghard, M. *Small* **2005**, *1*, 180−192. (g) Tasis, D.; Tagmatarchis, N.; Bianco, A.; Prato, M. *Chem. Rev.* **2006**, *106*, 1105−1136. (h) Dyke, C. A.; Tour, J. M. *Chem. Eur. J.* **2004**, *10*, 812−817.

(5) Britzab, D. A.; Khlobystov, A. N. *Chem. Soc. Rev.* **2006**, *35*, 637−659.

(6) Guldi, D. M.; Rahman, G. M. A.; Zerbetto, F.; Prato, M. *Acc. Chem. Res.* **2005**, *38*, 871−878.

(7) Kamat, P. V. *nanotoday* **2006**, *1*, 20−27.

(8) (a) Murakami, H.; Nomura, T.; Nakashima, N. *Chem. Phys. Lett.* **2003**, *378*, 481−485. (b) Li, H.; Zhou, B.; Lin, Y.; Gu, L.; Wang, W.; Fernando, K. A. S.; Kumar, S.; Allard, L. F.; Sun, Y.-P. *J. Am. Chem. Soc.* **2004**, *126*, 1014−1015. (c) Rahman, G. M. A.; Guldi, D. M.; Campidelli, S.; Prato, M. *J. Mater. Chem.* **2006**, *16*, 62−65. (d) Hasobe, T.; Fukuzumi, S.; Kamat, P. V. *J. Am. Chem. Soc.* **2005**, *127*, 11884−11885. (e) Chen, J.; Collier, C. P. *J. Phys. Chem. B* **2005**, *109*, 7605−7609. (f) Hasobe, T.; Fukuzumi, S.; Kamat, P. V. *J. Phys. Chem. B* **2006**, *110*, 25477−25484.;

(9) (a) Guldi, D. M.; Rahman, G. M. A.; Jux, N.; Tagmatarchis, N.; Prato, M. *Angew. Chem., Int. Ed.* **2004**, *43*, 5526−5530. (b) Guldi, D. M.; Rahman, G. M. A.; Jux, N.; Balbinot, D.; Tagmatarchisc, N.; Prato, M. *Chem. Commun.* **2005**, 2038−2040. (c) Ehli, C.; Rahman, G. M. A.; Jux, N.; Balbinot, D.; Guldi, D. M.; Paolucci, F.; Marcaccio, M.; Paolucci, D.; Melle-Franco, M.; Zerbetto, F.; Campidelli, S.; Prato, M. *J. Am. Chem. Soc.* **2006**, *128*, 11222−11231. (d) Guldi, D. M.; Rahman, G. M. A.; Jux, N.; Balbinot, D.; Hartnagel, U.; Tagmatarchis, N.; Prato, M. *J. Am. Chem. Soc.* **2005**, *127*, 9830−9838.

(10) Guldi, D. M.; Rahman, G. N. A.; Ramey, J.; Marcaccio, M.; Paolucci, D.; Paolucci, F.; Qin, S.; Ford, W. T.; Balbinot, D.; Jux, N.; Tagmatarchis, N.; Prato, M. *Chem. Commun.* **2005**, 2034−2035

(11) Richter, E.; Subbaswamy, K. R. *Phys. Rev. Lett.* **1997**, *79*, 2738−2741.

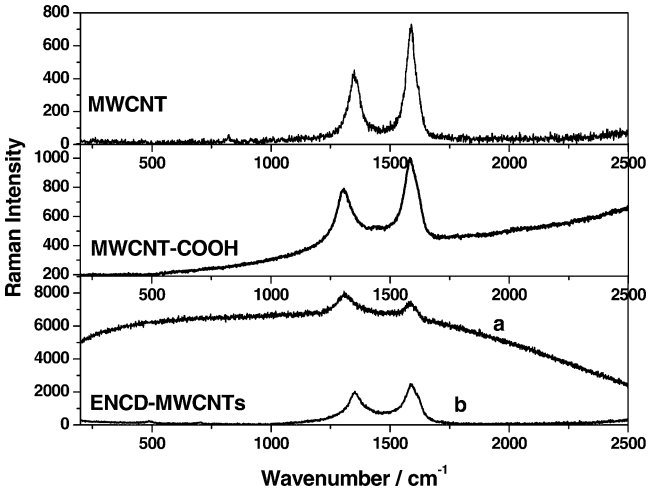

FIGURE 1. Raman spectra (excited with 785 nm laser) of MWCNTs, MWCNT-COOH, and ENCD-MWCNTs before (a) and after (b) thermal defunctionalization in a TGA scan to 450 °C.

COOH significantly shifts to lower wavenumbers by 43 cm^{-1} from 1350 to 1307 cm^{-1} after oxidation. Meanwhile, the relative intensity of the D band is significantly increased. I_D/I_G increases from 0.62 for raw MWCNTs to 0.79 for MWCNT-COOH. The relative intensity increase of the D band can be attributed to an increased number of sp^3-hybridized carbons in the nanotube framework, which demonstrates that the MWCNT-COOH shows a larger number of defects than the pristine MWCNTs. The peak in the 1500−1600 cm^{-1} region is the so-called G-band, which is the Raman-allowed phonon high-frequency E_{2g} first-order mode. The frequency of the G-band of MWCNT-COOH shows no significant shift. These results are indicative of covalent functionalization.[12−14] Comparing the spectra of MWCNT-COOH and ENCD-MWCNTs, the frequencies of the D and G bands undergo no significant shifts, which implies that the reaction of ENCD with MWCNT-COOH does not occur between the sidewall and ENCD. The control experiment also confirmed that no product was obtained after the reaction of ENCD with pristine MWCNTs. However, the ratio of the relative intensities of the D and G bands increases, which may be attributed to the strong luminescence from ENCD-MWCNTs.[15] Because the luminescence can be suppressed in defunctionalized nanotube samples,[15d] ENCD-MWCNTs were first thermally defunctionalized in a TGA scan to 450 °C, and then the rest of the sample was used for the Raman spectrum (Figure 1). The I_D/I_G ratio is ca. 0.81. The value is comparable to that of the MWCNT-COOH. The Raman results confirm that ENCD-MWCNTs contain functionalized MWCNTs.

X-ray Photoelectron Spectroscopy. XPS can provide chemical bonding information and is a useful technique for surface analysis. XPS was performed on MWCNT-COOH (Figure 2)

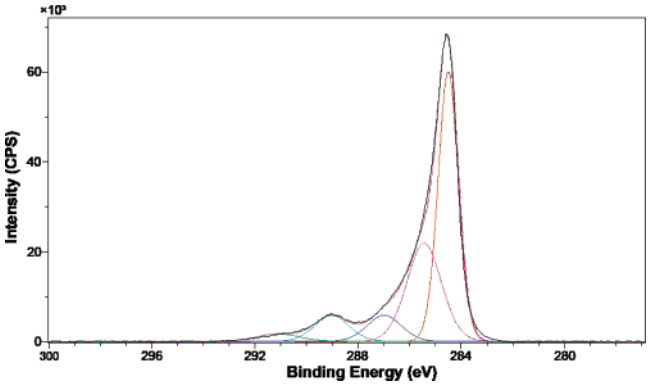

FIGURE 2. XPS C1s spectra of MWCNT-COOH. The black traces and the colored traces are experiment and fit results, respectively.

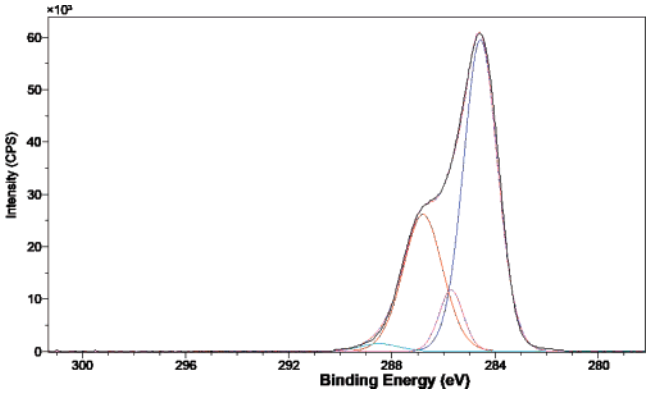

FIGURE 3. XPS C1s spectra of ENCD-MWCNTs. The black traces and the colored traces are experiment and fit results, respectively.

and ENCD-MWCNTs (Figure 3) to obtain the information about the functional groups on the nanotube surface. The C1s spectrum of MWCNT-COOH clearly consists of at least five components (284.5, 285.4, 287.0, 289.0, and 291.1 eV). That of ENCD-MWCNTs clearly consists of at least four components (284.6, 285.7, 286.8, and 288.5 eV). As is well-known, graphite exhibits an asymmetric peak centered at 284.66 eV with a long tail extended to the higher energy region.[16] The asymmetric peak was also observed for MWCNT-COOH and ENCD-MWCNTs, centered at 284.5 and 284.6 eV, which originates both in sp^2-hybryidized graphite-like carbon atoms and in carbon atoms bound to hydrogen atoms. The main peak at 285.4 and 285.7 eV can be assigned to sp^3-hybridized carbon atoms as in diamond-like carbon. The other three peaks of the C1s spectrum of MWCNT-COOH were assigned to −C═O (287.0 eV), −COOH (289.0 eV), and sp^2-hybryidized carbon π←π shakeup (291.1 eV), respectively. The other two peaks of the C1s spectrum of ENCD-MWCNTs were assigned to −C═O (286.8 eV), and −CO−NH (288.5 eV), respectively,[17] but the shakeup peak (291.1 eV) is absent after the surface of the MWCNT-COOH was attached by ENCD. The phenomenon that no shakeup is visible for ENCD-MWCNTs could be attributed to cyclodextrin's close contact with the surface of MWCNTs, as is that of the CNTs in the mixture.[18] Furthermore the XPS data provide an estimate of the degree of functionlization via the comparison of the amount of nitrogen and carbon (N-to-C ratio, 0.26%) in ENCD-MWCNTs. The average degree of function-

(12) Bahr, J. L.; Tour, J. M. *Chem. Mater.* **2001**, *13*, 3823−3824.
(13) Bahr, J. L.; Tour, J. M. *J. Mater. Chem.* **2002**, *12*, 1952−1958.
(14) Dyke, C. A.; Tour, J. M. *J. Am. Chem. Soc.* **2003**, *125*, 1156−1157.
(15) (a) Chattopadhyay, D.; Galeska, I.; Papadimitrakopoulos, F. *J. Am. Chem. Soc.* **2003**, *125*, 3370−3375. (b) Zhao, B.; Hu, H.; Niyogi, S.; Itkis, M. E.; Hamon, M. A.; Bhowmik, P.; Meier, M. S.; Haddon, R. C. *J. Am. Chem. Soc.* **2001**, *123*, 11673−11677. (c) Lin, Y.; Taylor, S.; Huang, W.; Sun, Y.-P. *J. Phys. Chem. B* **2003**, *107*, 914−919. (d) Riggs, J. E.; Guo, Z.; Carroll, D. L.; Sun, Y.-P. *J. Am. Chem. Soc.* **2000**, *122*, 5879−5880. (e) Huang, W.; Taylor, S.; Fu, K.; Lin, Y.; Zhang, D.; Hanks, T. W.; Rao, A. M.; Sun, Y.-P. *Nano Lett.* **2002**, *2*, 311−314.
(16) Th, P. M.; Attekum, M.; Wetheim, G. K. *Phys. Rev. Lett.* **1979**, *43*, 1896−1898.

alization determined is less than 0.07% addend per C-atom of the tube sidewalls (atom %).[19]

TG and DTA. The thermal behavior of the ENCD-MWCNTs, along with their constituent parts, was studied from room temperature to 800 °C in flowing oxygen. ENCD starts losing weight at 228 °C and loses 96% of its original weight at 557 °C. The two decomposition points of 228 and 314 °C correspond to the loss of the aminoethylene amino group and cyclodextrin backbone, respectively. The decomposition point of MWCNTs is at 565 °C, and 98% of its original weight is lost at 600 °C. However, for the conjugate of ENCD and MWCNTs, the corresponding temperature is lower than that of the naked MWCNTs but higher than that of ENCD. Hence, we can deduce that the thermal stability of MWCNTs reduce after being modified by ENCD.

Fluorescence Spectroscopy. As is well-known, electron-transfer reactions take place between carbon nanotubes and covalent or noncovalent porphyrins.[6,8,9,20] Fluorescence spectroscopy is proven to be a sensitive tool for the investigation of the electron donor and acceptor interactions. Upon addition of the ENCD-MWCNTs, the fluorescence of TCPP (Figure 4) and ZnTCPP (Figure 5) were both quenched about 70% at 644 and 607 nm, respectively. The extent of fluorescence quenching upon adding the MWCNT-COOH solution is the same as when adding ENCD-MWCNTs. The fluorescence intensity of TCPP in the aqueous solution was slightly enhanced by the addition of β-CD,[21] indicating that the fluorescence quenching of the TCPP is not electron transfer between the TCPP and the ENCD when in the cavity, so the quenching process was attributed to PET between MWCNTs and TCPP or ZnTCPP. However, it was absolutely different in DMF solution. Upon adding the DMF solution of MWCNT-COOH, the fluorescence of ZnTCPP was quenched about 60%, which is similar to the aqueous solution. Upon adding the DMF solution of ENCD-MWCNTs, the fluorescence intensity of ZnTCPP was hardly decreased. So we can deduce that TCPP or ZnTCPP was included in the cavities of the CD of ENCD-MWCNTs in the aqueous solution, and

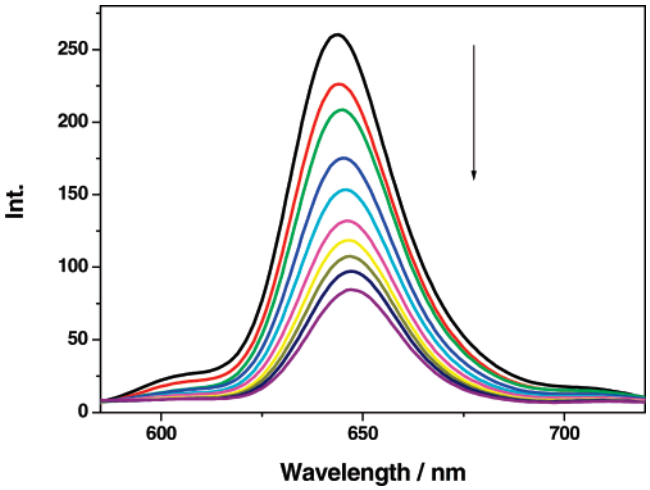

FIGURE 4. Fluorescence spectral changes of TCPP (1.225×10^{-6} M) upon gradual addition of ENCD-MWCNTs (0−86.4 μg/mL) in a Tris 8.0 buffer solution at 298 K (excitation wavelength 414 nm, excitation and emission slit width of 10 nm).

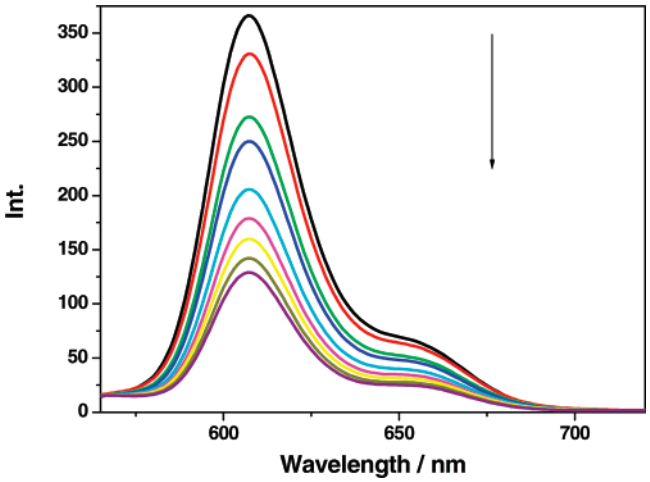

FIGURE 5. Fluorescence spectral changes of ZnTCPP (1.416×10^{-6} M) upon gradual addition of ENCD-MWCNTs (0−86.4 μg/mL) in a Tris 8.0 buffer solution at 298 K (excitation wavelength 422 nm, excitation and emission slit width of 10 nm).

the electron transfer from porphyrin to MWCNTs took place as a consequence of this. While in DMF solution, for the CD attaching on the surface of MWCNTs, PET was prevented because of DMF excluding the TCPP from the CD cavity. However, comparing the quencher concentrations and the quenching ratio in aqueous solutions, the presence of the CD on the surface decreased the quenching efficiency of MWCNTs and partly disrupted the PET process. Interestingly, preferential quenching of the fluorescence of ZnTCPP occurs upon addition of ENCD-MWCNTs, while fluorescence recovery can be achieved when the added 1-adamantane acetic acid (1-ADA) rejects ZnTCPP from cavities of CD of ENCD-MWCNTs (Figure 6). The PET process was reversible and controllable by inclusion in the cavities of the CD and by the solvent after the CD was introduced on the surface of MWCNTs.

Fluorescence Decay. Prior to the addition of ENCD-MWCNTs, the fluorescence decay of ZnTCPP is mono-exponential, from which a lifetime of 2.2 ns was determined. After addition of MWCNT-COOH, the fluorescence decay is bi-exponential, and the two corresponding lifetimes are 0.2 and

(17) (a) Chattopadhyay, J.; de Jesus Cortez, F.; Chakraborty, S.; Slater, N. K. H.; Billups, W. E. *Chem. Mater.* **2006**, *18*, 5864−5868. (b) Ago, H.; Kugler, T.; Cacialli, F.; Salaneck, W. R.; Shaffer, M. S. P.; Windle, A. H.; Friend, R. H. *J. Phys. Chem. B* **1999**, *103*, 8116−8121. (c) Luong, J. H. T.; Hrapovic, S.; Liu, Y.; Yang, D.-Q.; Sacher, E.; Wang, D.; Kingston, C. T.; Enright, G. D. *J. Phys. Chem. B* **2005**, *109*, 1400−1407. (d) Peng, Y.; Liu, H. *Ind. Eng. Chem. Res.* **2006**, *45*, 6483−6488. (e) Okpalugo, T. I. T.; Papakonstantinou, P.; Murphy, H.; McLaughlin, J.; Brown, N. M. D. *Carbon* **2005**, *43*, 153−161. (f) Urszula, D. W.; Viera, S.; Ralf, G.; Sung, H. J.; Byung, H. K.; Hyun, J. L.; Lothar, L.; Yung, W. P.; Savas, B.; David, T.; Siegmar, R. *J. Am. Chem. Soc.* **2005**, *127*, 5125−5131. (g) Lee, W. H.; Kim, S. J.; Lee, W. J.; Lee, J. G.; Haddon, R. C.; Reucroft, P. J. *Appl. Surf. Sci.* **2001**, *181*, 121−127.

(18) (a) Yang, D.-Q.; Sacher, E. *Surf. Sci.* **2002**, *504*, 125−137. (b) Yang, D.-Q.; Sacher, E. *Surf. Sci.* **2002**, *516*, 43−55. (c) Yang, D.-Q.; Rochette, J.-F.; Sacher, E. *J. Phys. Chem. B* **2005**, *109*, 4481−4484.

(19) Holzinger, M.; Abraham, J.; Whelan, P.; Graupner, R.; Ley, L.; Hennrich, F.; Kappes, M.; Hirsch, A. *J. Am. Chem. Soc.* **2003**, *125*, 8566−8580.

(20) (a) Baskaran, D.; Mays, J. W.; Zhang, X. P.; Bratcher, M. S. *J. Am. Chem. Soc.* **2005**, *127*, 6916−6917. (b) Guldi, D. M.; Marcaccio, M.; Paolucci, D.; Paolucci, F.; Tagmatarchis, N.; Tasis, D.; Vázquez, E.; Prato, M. *Angew. Chem., Int. Ed.* **2003**, *42*, 4206−4209. (c) Guldi, D. M.; Taieb, H.; Rahman, G. N. A.; Tagmatarchis, N.; Prato, M. *Adv. Mater.* **2005**, *17*, 871−875. (d) Campidelli, S.; Sooambar, C.; Lozano-Diz, E.; Ehli, C.; Guldi, D. M.; Prato, M. *J. Am. Chem. Soc.* **2006**, *128*, 12544−12552. (e) Cioffi, C.; Campidelli, S.; Sooambar, C.; Marcaccio, M.; Marcolongo, G.; Meneghetti, M.; Paolucci, D.; Paolucci, F.; Ehli, C.; Rahman, G. M. A.; Sgobba, V.; Guldi, D. M.; Prato, M. *J. Am. Chem. Soc.* **2007**, *129*, 3938−3945.

(21) Hamai, S.; Ohshida, T. *J. Inclusion Phenom. Macrocyclic Chem.* **2004**, *50*, 209−217.

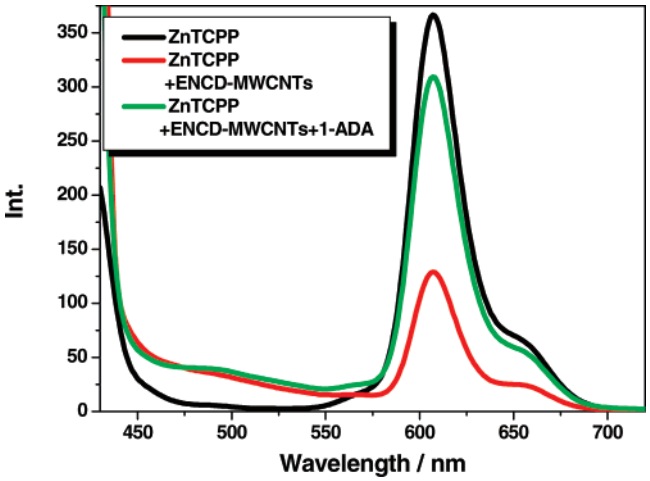

FIGURE 6. Fluorescence spectral changes of ZnTCPP (1.307×10^{-6} M) upon subsequent addition of ENCD-MWCNTs (76.8 μg/mL) and 1-ADA (3.091×10^{-5} M) in a Tris 8.0 buffer solution (excitation wavelength 422 nm, excitation and emission slit width of 10 nm).

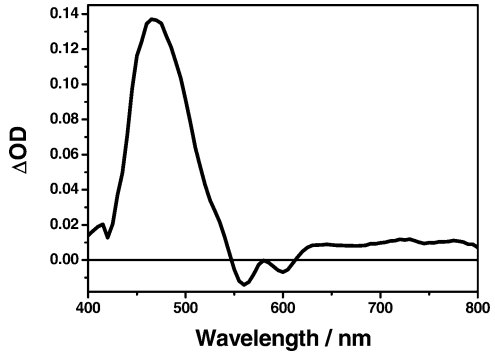

FIGURE 7. Transient absorption spectrum obtained upon nanosecond flash photolysis (532 nm) of ZnTCPP/ENCD-MWCNTs in nitrogen saturated solutions with a time delay of 100 ns.

2.2 ns, respectively. In sharp contrast, the fluorescence decay of ZnTCPP becomes tri-exponential with the addition of ENCD-MWCNTs, and the corresponding lifetimes are 0.2, 2.2, and 6.7 ns, respectively. These imply that the fast decaying component (0.2 ns) corresponds to the intermolecular electron-transfer quenching within both ZnTCPP/MWCNT-COOH and ZnTCPP/ENCD-MWCNTs systems, while the slower decaying component (2.2 ns) represents deactivation in free ZnTCPP. For the ZnTCPP/ENCD-MWCNTs system, the longest lifetime (6.7 ns) is attributed to the electron-transfer quenching between ZnTCPP inside the cyclodextrin on ENCD-MWCNTs and MWCNTs. Comparing ZnTCPP/MWCNT-COOH and ZnTCPP/ENCD-MWCNTs, the extra slowest decaying component (6.7 ns) in ZnTCPP/ENCD-MWCNTs would reduce the quenching efficiency. The observations are well consistent with the above results of the fluorescence experiments.

Transient Absorption Spectroscopy. Another spectroscopic observation in support of a successful electron-transfer quenching comes from transient absorption measurements following 532 nm laser excitation. The transient of the photoproduct is illustrated in Figure 7. A stable transient maximum develops at 470 nm. It was flanked by fluorescence-stimulated bleaching between 500 and 600 nm. One important feature is the broad absorption between 600 and 800 nm, which should be attributed to the one-electron-oxidized π-radical cation of ZnTCPP, i.e., $ZnTCPP^{+\bullet}$. This observation implies an electron-transfer product that evolves from a photoinduced electron transfer between the photoexcited ZnTCPP and ENCD-MWCNTs.[6,8−10,20,22]

Cyclic Voltammetry. The electrochemical behavior of ZnTCPP, TCPP, TCPP/ENCD-MWCNTs, and ZnTCPP/ENCD-MWCNTs was investigated in aqueous solution, with KCl as the supporting electrolyte. The experiments were performed with a wide potential window to obtain a thorough characterization of the redox process. The curve for free TCPP displays a distinct reduction peak, with the peak potential at 933 mV. In comparison to the CV behavior of free TCPP, the cyclic voltammetric scan for TCPP displays the reduction potential at 875 mV upon addition of ENCD-MWCNTs. Such processes are associated with one-electron transfers localized on the porphyrin moieties and such a shift can likely to be attributed to the strong electronic interaction between ENCD-MWCNTs and TCPP. The same conclusion was obtained from the cyclic voltammetric scan of ZnTCPP in the absence and presence of ENCD-MWCNTs.

Conclusion

A conjugate of ENCD and MWCNTs was successfully prepared with the modification of surface of MWCNTs. The introduction of the CDs efficiently increased the water solubility. Upon addition of the ENCD-MWCNTs, the fluorescence of porphyrins was quenched as a result of the PET process between porphyrins and MWCNTs. The fluorescence recovery can be achieved in the presence of 1-ADA by rejecting porphyrins from the cavities of CDs of ENCD-MWCNTs. In the DMF solution, the fluorescence intensity of porphyrins was hardly decreased upon the addition of ENCD-MWCNTs. The observations indicate that the CD cavities play a vital role in the control of the PET process. Benefiting from the fascinating functions of porphyrins and carbon nanotubes, the materials will most likely have future applications in many fields of chemistry and photovoltaic materials.

Experiment Section

MWCNTs produced by the CVD method were obtained from Chengdu Organic Chemistry Co., Ltd, Chinese Academy of Sciences. Surface-bound carboxylic acid groups of MWCNTs (MWCNT-COOH),[23] 6^{I}-(2-aminoethyleneamino)-6^{I}-β-deoxycyclodextrin (ENCD),[24] tetrakis(4-carboxyphenyl)porphyrin (TCPP),[25] and zinc tetrakis(4-carboxyphenyl)porphyrin (ZnTCPP)[26] were prepared according to literature procedures.

Fluorescence spectra were recorded in a conventional quartz cell (10 mm × 10 mm × 45 mm) at 25 °C on a JASCO FP-750 fluorescence spectrometer with the excitation and emission slits of 10 nm width. Fluorescence lifetimes were measured with an Edinburgh Analytical Instruments FL900CD spectrometer employing the time correlated single photon counting technique. Nanosecond pulsed excitation was carried out with an nF-900 flash lamp filled with ultrapure hydrogen (0.4 bar, 40 kHz repetition rate).

(22) (a) Guldi, D. M. *Chem. Soc. Rev.* **2002**, *31*, 22−36. (b) Balbinot, D.; Atalick, S.; Guldi, D. M.; Hatzimarinaki, M.; Hirsch, A.; Jux, N. *J. Phys. Chem. B* **2003**, *107*, 13273−13279. (c) Guldi, D. M.; Rahman, G. M. A.; Sgobba, V.; Ehli, C. *Chem. Soc. Rev.* **2006**, *35*, 471−487.

(23) Li, S.; Qin, Y.; Shi, J.; Guo, Z.-X.; Li, Y.; Zhu, D. *Chem. Mater.* **2005**, *17*, 130−135.

(24) May, B. L.; Kean, S. D.; Easton, C. J.; Lincoln, S. F. *J. Chem. Soc., Perkin Trans. 1* **1997**, 3157−3160.

(25) Datta-Gupta, N.; Bardos, T. *J. Heterocycl. Chem.* **1966**, *3*, 495−502.

(26) Dabestani, R.; Bard, A. J.; Campion, A.; Fox, M. A.; Mallouk, T. E.; Webber, S. E.; White, J. M. *J. Phys. Chem.* **1988**, *92*, 1872−1878.

No polarizers were used. The signal was detected by a red-sensitive Peltier system cooled S900 single photon photomultiplier detection system. The fluorene chromophores were excited at 414 and 422 nm, and time-resolved fluorescence decays were recorded on a time scale of 50−200 ns, resolved into 1024 channels, to a total of 10 000 counts in the peak channel by collecting emission at 644 and 607 nm, with a bandwidth of 18 nm. Decay curves were analyzed by using a standard iterative reconvolution method in the F900 software packages. A multiexponential decay function was assumed:

$$R(t) = A + \sum_{i=1}^{4} B_i \, e^{-t/\tau i}$$

where B_i are pre-exponential factors, τ_i are the characteristic lifetimes, and A is an additional background factor. The cyclic voltammetry (CV) measurements were performed on a BAS Epsilon electrochemical analyzer in a deoxygenated aqueous solution containing 0.10 M KCl as a supporting electrolyte at 298 K (50 mV s^{-1}). The glassy carbon working electrode was polished with BAS polishing alumina suspension and rinsed with acetone before use. The counter electrode was a platinum wire. The measured potentials were recorded with respect to an Ag/AgCl (3 M NaCl) reference electrode. Nanosecond transient absorption spectra were performed on a LP-920 pump−probe spectroscopic setup. The excited source was the unfocused third harmonic 532 nm output of a Nd:YAG laser (10 Hz, 8 ns) (Continuum surelite II); the probe light source was a pulse-xenon lamp. The signals were detected by Edinburgh analytical instruments (LP900) and recorded on a Tektronix TDS 3012B oscilloscope and a computer.

Preparation of the ENCD-MWCNTs. MWCNT-COOH (20 mg) was treated with thionyl chloride and then reacted with 100 times excess ENCD in 50 mL of DMF at 90 °C for 7 days under a pure nitrogen atmosphere. The solvent was removed under reduced pressure and 120 mL of water/ethanol (1:2.5) was added to remove unreacted ENCD. The mixture was stirred for several hours at room temperature. After collection via centrifugation, the crude product obtained was dried in vacuo to give a black solid of the ENCD-MWCNTs conjugate (19.0 mg).

Acknowledgment. This work is supported by the 973 Program (2006CB932900), TNSF **(**07QTPTJC29700), NNSFC (nos. 20421202 and 20572052), and the Program for New Century Excellent Talents in University (NCET-05-0222). We would like to thank Prof. Vernon D. Parker at Utah State University for assistance in the preparation of this manuscript. We also thank Dr. Steffen Jockusch and Dr. Xiaopeng Bai in Chemistry Department at Columbia University for their discussion in the fluorescence spectroscopy.

Supporting Information Available: FT-IR, TG-DTA, XPS spectrum, fluorescence titration spectra, and cyclic voltammetric scans. This material is available free of charge via the Internet at http://pubs.acs.org.

JO702400K